

Light Water Reactor Sustainability Program:

Report Summarizing the Status of Second Round Irradiation Experiments and Assessment of Materials Available for Testing Advanced Welding Techniques

Milestone M3LW-17OR0406013

July 2017



This report was prepared as an account of work sponsored by an agency of the United States Government. Neither the United States Government nor any agency thereof, nor any of their employees, makes any warranty, express or implied, or assumes any legal liability or responsibility for the accuracy, completeness, or usefulness of any information, apparatus, product, or process disclosed, or represents that its use would not infringe privately owned rights. Reference herein to any specific commercial product, process, or service by trade name, trademark, manufacturer, or otherwise, does not necessarily constitute or imply its endorsement, recommendation, or favoring by the United States Government or any agency thereof. The views and opinions of authors expressed herein do not necessarily state or reflect those of the United States Government or any agency thereof.

Light Water Reactor Sustainability Program

Report Summarizing the Status of Second Round Irradiation Experiments and Assessment of Materials Available for Testing Advanced Welding Techniques

Zhili Feng, Roger Miller, Nesrin Cetiner¹ and Xunxiang Hu

Materials Science and Technology Division

¹ Reactor and Nuclear Systems Division

Scarlett Clark

Fusion and Materials for Nuclear Systems

Oak Ridge National Laboratory

Gregory Frederick, Benjamin Sutton

Welding and Repair Technology Center

Electric Power Research Institute

Date Published: July 2017

Prepared under the direction of the
U.S. Department of Energy
Office of Nuclear Energy
Light Water Reactor Sustainability Program
Materials Aging and Degradation Pathway

Prepared by
OAK RIDGE NATIONAL LABORATORY
Oak Ridge, Tennessee 37831
managed by
UT-BATTELLE, LLC
for the
U.S. DEPARTMENT OF ENERGY
under contract DE-AC05-00OR2272

THIS PAGE IS INTENTIONALLY BLANK

EXECUTIVE SUMMARY

Welding is widely used for repair, maintenance and upgrade of nuclear reactor components. As a critical mitigation technology to extend the service life of nuclear power plants beyond 60 years, weld technology must be further developed to avoid and/or reduce the detrimental effect associated with the traditional welding fabrication practices, as well as for the ability to repair of highly irradiated materials. As nuclear power plants age, the extent and level of radiation damage will increase, as does the demand of welding repair and mitigation of irradiated structural internals.

This research is a joint DOE/LWRSP (Light Water Reactor Sustainability Program) and EPRI/LTO (Long Term Operability) effort aimed at developing advanced welding technology for reactor repair and upgrade. It focuses on welding repair of irradiated materials that are extremely challenging and requires long-term research and development. The technology development is also expected to have broad benefit. For example, the proactive stress management and friction stir welding technology can improve the resistance to stress corrosion cracking. The advanced welding simulation tool would provide more reliable prediction of the weld residual stress for component integrity analysis and risk assessment. The DOE LWRSP portion of the project will focus on the fundamental science aspect of the project, whereas the EPRI/LTO part will focus on the welding system and process development.

This milestone was directed toward continued production of helium containing materials representative of those expected in a nuclear power plant reactor internals at extended service times, through neutron irradiation in the High Flux Isotope Reactor (HFIR) facility at Oak Ridge National Laboratory (ORNL). This report details information on: 1) the status of the second round of irradiations on specially prepared material (high initial boron concentrations) consisting of stainless steel alloys 304L and 316L and Nickel alloy 182; 2) status of the results from first round irradiations regarding helium levels and distribution of helium within the microstructures; and 3) status of planning and schedule for additional irradiations.

The second round of irradiation was completed on May 26, 2017 and consisted of 45 coupons with controlled boron doping in stainless steel alloys 304L, 316L and Nickel alloy 182. The helium bubble distribution within the materials irradiated in the first round of irradiation (2014) is being investigated through Transmission Electron Microscopy (TEM) and a limited number of samples have been tested. Thermal desorption spectrometry (TDS) technique was used to obtain the total amount of helium in the cold 304 stainless steel sample, which requires melting the sample of interest to release all the contained helium. This sample was supplied by EPRI and was produced by powder metallurgy and contained an unknown amount of helium. A new customized resistivity heater with a maximum temperature of 1650°C has been installed to the TDS system located in the low activation materials development and analysis lab at ORNL in order to enable melting of the metal samples.

The assessment of the total number of coupons available for welding and an evaluation by EPRI on potential levels of existing reactor materials and radiation history indicated that production of additional coupons is needed and that it was advisable to produce coupons with even higher helium levels than produced in the past. A campaign was started to produce four additional material heats that that will provide additional coupons of previously made material plus two heats of material with higher helium generation potential that will be irradiated at a future date in the HFIR facility.

Producing Boron Containing Alloys

Repair welding on highly irradiated helium-containing materials can lead to cracking in the heat-affected zone (HAZ) of the weld region. Studies in the past have established that such cracking is attributed to the presence of entrapped helium in the post-irradiated material. Helium forms by transmutation of boron and nickel into alpha particles under neutron irradiation, as illustrated in Figure 1(a). Helium is essentially insoluble in metals. It is therefore thermodynamically favorable for the entrapped helium to precipitate to form bubbles/microvoids/cavities along grain boundaries. Helium bubbles nucleate, grow and coalesce rapidly at grain boundaries under the combined actions of high temperature and tensile stresses, which occur during the welding process. Intergranular rupture occurs as the cohesive strength of the grain boundary (weakened by helium bubbles) can no longer bear the shrinkage-induced internal tensile stress during cooling of the weld. Cracks form primarily in the HAZ, generally less than a millimeter from the fusion boundary. An example of helium induced weld cracking is shown in Figure 1(b). The production of the helium containing materials consisted of (1) producing custom made alloys of precisely controlled chemistries with controlled additions of boron at several target levels, and (2) irradiating the boron containing alloys with neutrons to transmute boron (and a small amount of Ni) to helium. Such an elaborate strategy, although expensive, was essential to produce alloys closely subjecting to the helium generation processes in a nuclear reactor necessary for the planned welding repair study.

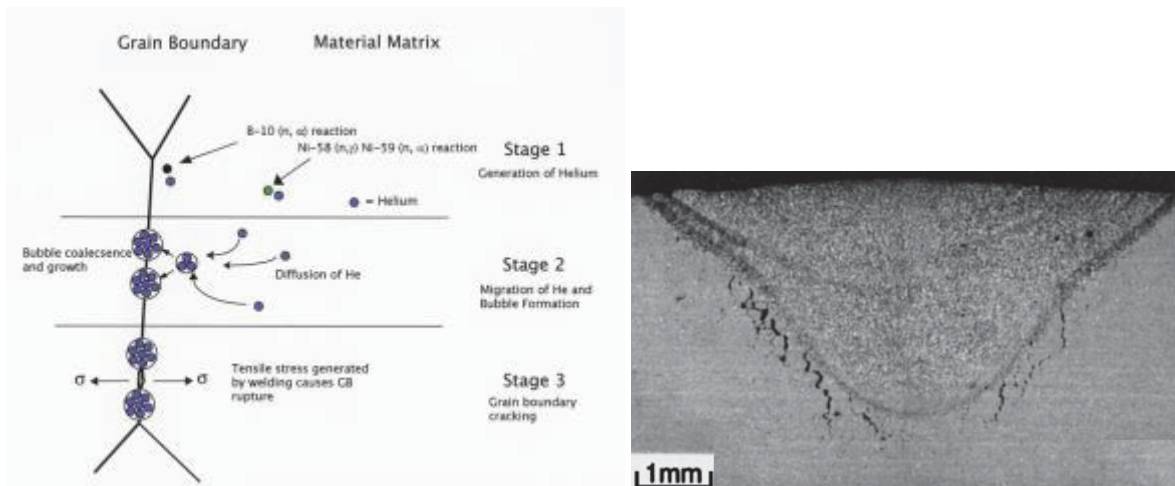


Figure 1. (a) Formation of helium due to transmutation of B and Ni from neutron irradiation. (b) Helium induced cracking in a TIG weld of stainless steel SUS304 (after Asano et al, (1999) J. Nuclear Materials, 264:1-9)

The two stainless steels alloys (304L and 316L) were produced at ORNL in 2013 to produce the initial material heats for irradiation. Five heats of each alloy were doped with natural occurring boron at five different concentration levels (nominally 1, 5, 10, 20 and 30 ppm natural boron by weight) and casted by Vacuum Arc Remelting (VAR) followed by extrusion at 1100°C through a 19 by 51 mm rectangular die. The ingots were then homogenized at 1100°C for 5 hours in air and then hot rolled to 19 mm thick, followed with cold rolling to 12 mm thick (about 35% reduction) to produce rectangular bar stock. A solution heat treatment (1000°C for 30 minutes for 304L and 1050°C for 30 minutes for 316L followed by water quenching) was then applied to produce acceptable microstructure. Metallographic characterization confirmed that both alloys had satisfactory grain size (less than 100 micron), absence of grain boundary carbides, and acceptable ferrite and martensite levels. The bar stock was machined to final dimensions (76x56x8.9mm nominal) to yield 6-8 pieces at each boron level for subsequent irradiation.

Table 1 shows the complete chemistry analysis results of the ten heats of stainless steel made in this project to date. As shown in the table, the target boron concentrations were achieved. Furthermore, cobalt (Co) concentrations in all samples were extremely low, in the range of 60-80 ppm by weight. It was done deliberately through an exhaustive search of low cobalt (Co) master alloys used in the VAR process. The Co concentrations were kept as low as practically possible, in order to minimize the radiation level of the specimens to ease the handling and analysis of irradiated materials during the repair welding experiment and post welding analysis and characterization. Elements listed in ppm units were analyzed by Glow Discharge Mass Spectrometry (GDMS) while elements listed by weight percent (wt%) were analyzed by Optical Emission Spectrometry (OES) with the exception of carbon (Leco Combustion) and nitrogen (Gas Fusion). Elements listed twice were analyzed by both methods.

Five heats of Alloy 182 with five boron target concentration levels (nominally 1, 5, 10, 20, and 30 ppm boron by weight) were produced by Sophisticated Alloys, Inc. in 2013 following specifications provided by ORNL. Table 2 shows the complete chemistry analysis of the Alloys 182 heats made in this project. As shown in the Table 2 not all of the target boron concentrations were achieved but a wide range of boron levels were produced ranging from 0.3 to 23 ppm. All other elements met the chemistry requirements for Alloy 182. As with the stainless steel, the Co concentrations were kept as low as practically possible, in order to minimize the radiation level of the specimens to ease the handling and analysis of irradiated materials during the repair welding experiment and post welding analysis and characterization. Bar stock sections machined to final dimensions (76x56x8.9mm nominal) to yield 7 pieces at each boron level for subsequent irradiation. These thirty-five specimens have a wrought microstructure similar to the stainless steel specimens. Alloy 182, being weld filler metal, typically has a coarser weld microstructure in reactor structures. An additional fifteen specimens from heats 182D and 182E respectively, were fusion welded on one side to half of the specimen depth to produce a representative weld microstructure.

Table 1. Chemistry Analysis Results of 304L and 316L produced at ORNL

Element	Unit	Stainless Steel Heat Identification									
		304A	304B	304C	304D	304E	316A	316B	316C	316D	316E
B	ppm	0.8	4.8	10	24	32	0.9	4.7	12	22	30
Co	ppm	77	79	79	75	76	68	70	64	69	65
Al	ppm	5	5	4	10	5	4	5	6	4	4
P	ppm	18	19	19	18	18	16	17	28	16	14
S	ppm	14	14	14	15	14	14	14	23	14	13
Mo	ppm	390	220	180	240	180					
Cu	ppm	600	590	610	590	600	530	540	570	530	520
C	wt.%	0.012	0.007	0.014	0.01	0.012	0.012	0.012	0.014	0.007	0.009
Mn	wt.%	1.54	1.55	1.5	1.53	1.52	1.4	1.39	1.39	1.42	1.39
Si	wt.%	0.49	0.5	0.49	0.49	0.48	0.44	0.43	0.43	0.44	0.42
P	wt.%	<0.001	<0.001	<0.001	<0.001	<0.001	<0.001	<0.001	0.001	<0.001	<0.001
S	wt.%	0.002	0.003	0.002	0.002	0.002	0.002	0.002	0.004	0.001	0.002
Cr	wt.%	19.53	19.54	19.28	19.33	19.14	17.81	17.63	17.42	17.57	17.38
Ni	wt.%	10.61	10.52	10.35	10.41	10.25	12.08	11.82	11.83	11.88	11.92
Mo	wt.%	0.05	0.04	0.04	0.04	0.04	2.54	2.41	2.65	2.51	2.72
Cu	wt.%	0.05	0.05	0.05	0.05	0.05	0.05	0.05	0.06	0.06	
N	wt.%	0.035	0.032	0.035	0.035	0.035	0.03	0.03	0.034	0.031	0.03
Fe		Balance	Balance	Balance	Balance	Balance	Balance	Balance	Balance	Balance	Balance

Table 2. Chemistry Analysis Results of Alloy 182 produced by Sophisticated Alloys Inc.

Element	Unit	Alloy 182 Heat Identification				
		182A	182B	182C	182D	182E
B	ppm	0.3	5	15	14	23
Co	ppm	2	2	2	2	2
Al	ppm	81	34	32	54	56
Mo	ppm	1	1	8	1	1
Cu	ppm	2	1	2	1	1
C	wt%	0.03	0.08	0.03	0.04	0.04
Mn	wt%	7.03	7.00	6.76	7.17	7.08
Si	wt%	0.50	0.50	0.51	0.50	0.49
Cr	wt%	15.99	16.00	16.00	16.16	16.10
Fe	wt%	7.36	7.92	7.31	7.14	7.12
Nb	wt%	2.07	2.06	1.83	1.82	1.84
Ti	wt%	0.44	0.43	0.43	0.43	0.46
P	wt%	0.00013	0.00011	0.00018	0.00015	0.00016
S	wt%	0.00207	0.00199	0.00280	0.00200	0.00220
Ni		Balance	Balance	Balance	Balance	Balance

Second Irradiation Campaign

The second irradiation experiment was designed and conducted in the same manner as the first irradiation campaign conducted in 2014 and was completed in May 2017. Design changes were incorporated into the sample holder in order to make removal of the coupons easier for HFIR operations.

The first task involved identifying the irradiation locations at HFIR that can accommodate the fairly large specimens (by irradiation standards) necessary for repair welding studies. Through fitting tests, it was determined the four large bores labeled as VXF-16, VXF-17, VXF-19 and VXF-21 were suitable for the planned irradiation experiments as shown in Figure 2. The second irradiation used the same three large bore holes (VXF-16, VXF-17, VXF-19) as the first irradiation campaign in 2014.

The second task was detailed neutronics calculations to determine the amount of irradiation required to generate the targeted helium level in each specimen, to develop the layout of the specimen in each bore, and to ensure the safety margin to irradiate the specimens. After extensive neutronics calculations with different codes, the irradiation strategy was developed which requires completely transmuting boron to helium while keeping the transmutation of nickel to a minimal amount. This avoided the non-uniform generation of helium within a specimen, and also avoided variations of helium from one specimen to another, due to the non-uniform neutron flux of reactor core in the axial direction and the attenuation of neutrons by the specimen. This requires irradiating the specimens for three operating cycles at HFIR. The neutronics calculations and dosimetry results and analysis from the first irradiation campaign agreed very well and a decision was made to omit dosimetry from the second campaign. The results of the dosimetry analysis and calculations were detailed in ORNL Milestone Report MSLW-160R040615.

The third task was to design and build a special specimen holder/fixture to position the specimens in place during irradiation. Each holder can host up to 15 specimens in a 5x3 pattern. After the first irradiation campaign, it was difficult to remove the specimens from the holders. The holders were redesigned in two areas. The water flow channel was redesigned with corner relief slots to prevent sticking of the specimens to the holder when removing specimens while maintaining proper water flow. The second redesign incorporated a pull rod mechanism to allow specimens to be pulled from the holder if any specimen sticking still occurred. This mechanism was designed to operate within the dosimetry slots of the original design since neutronics calculations and dosimetry results had good agreement in the first campaign and no dosimetry was required for the second irradiation. A CAD drawing is shown in Figure 3 showing the general location of irradiation coupons and the pull rod mechanism. Figure 4 illustrates the specimen holder prior to loading, the general location where the specimens, and the height spacer to center the specimens at the reactor midplane. After assembly, the specimens and pull rod mechanism can be seen in Figure 5.

The orientation of the specimens relative to the fuel rods (neutron radiation source) is shown in Figure 6. As noted on this figure, the specimen closest to the reactor core is referred as the “front” or “towards or T” specimen while the specimen farthest from the reactor core is referred to as the “back” or “away or A” specimen. Information or data contained in this report may use either designation for location. It should be noted that there is about 10-20% flux variation along the length direction of the neutron source. There is also neutron flux decay due to the neutron attenuation caused by the specimen in front of it facing the

neutron source. These spatial variations of the neutron flux were addressed in the irradiation experiment procedure, as described above.

The loading diagram for each specimen holder, irradiation location and specimen identification for the second irradiation campaign is shown in Figure 7. Nickel 182 is a filler metal used in reactor construction particularly in dissimilar weld joints and the welding of nickel alloys. The Nickel 182 alloy produced by Sophisticated Alloys has a wrought microstructure rather than a coarser grain weld microstructure. EPRI performed welding on a number of coupons to produce the typical weld microstructure and re-machined the coupons to meet the requirements of the specimen holders. Both wrought and weld microstructures for nickel alloy 182 were included in the second irradiation campaign. This campaign was started with HFIR Fuel Cycle 470 (January 3, 2017) and concluded with HFIR Fuel Cycle 472 that finished on May 26, 2017. The three specimen holders were removed from the reactor and are presently stored in holding racks within the reactor pool. With the second irradiation campaign completed, ninety weld specimens are available for program use.

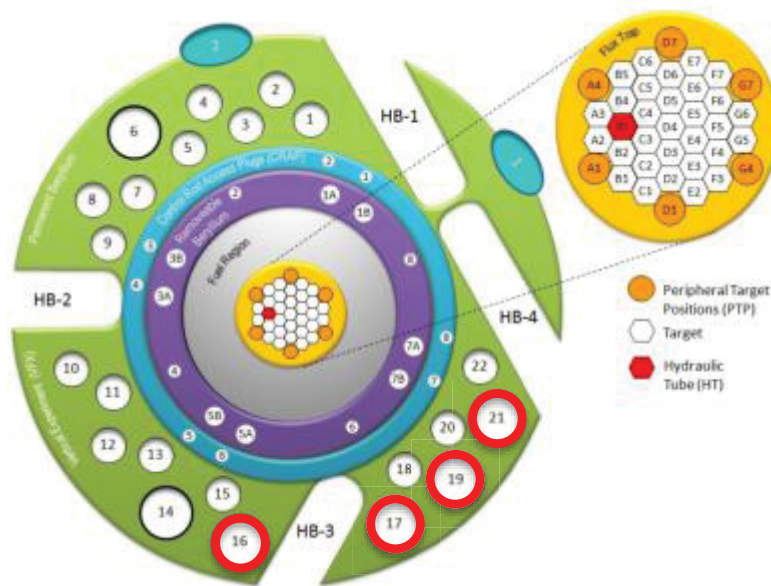


Figure 2. Locations of large bores (in red circles) at HFIR used for the irradiation experiments

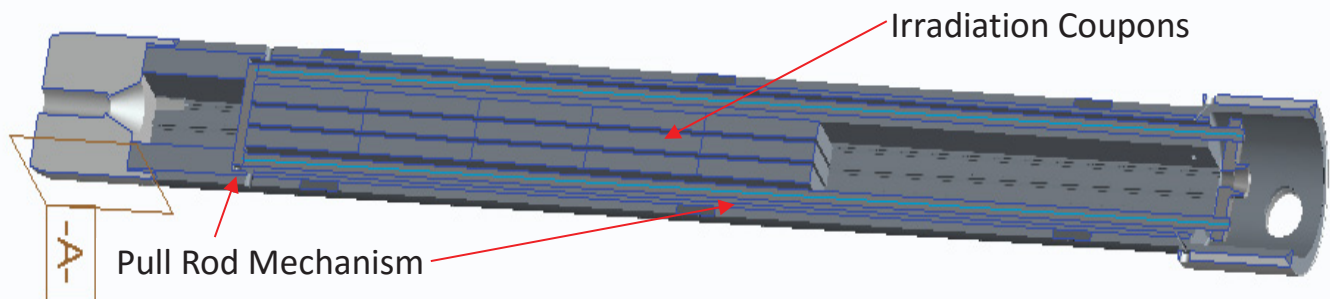


Figure 3. CAD drawing of the redesigned sample holder with pull rod mechanism



Figure 4. Photo of specimen holder, irradiation specimens and height spacer prior to final assembly

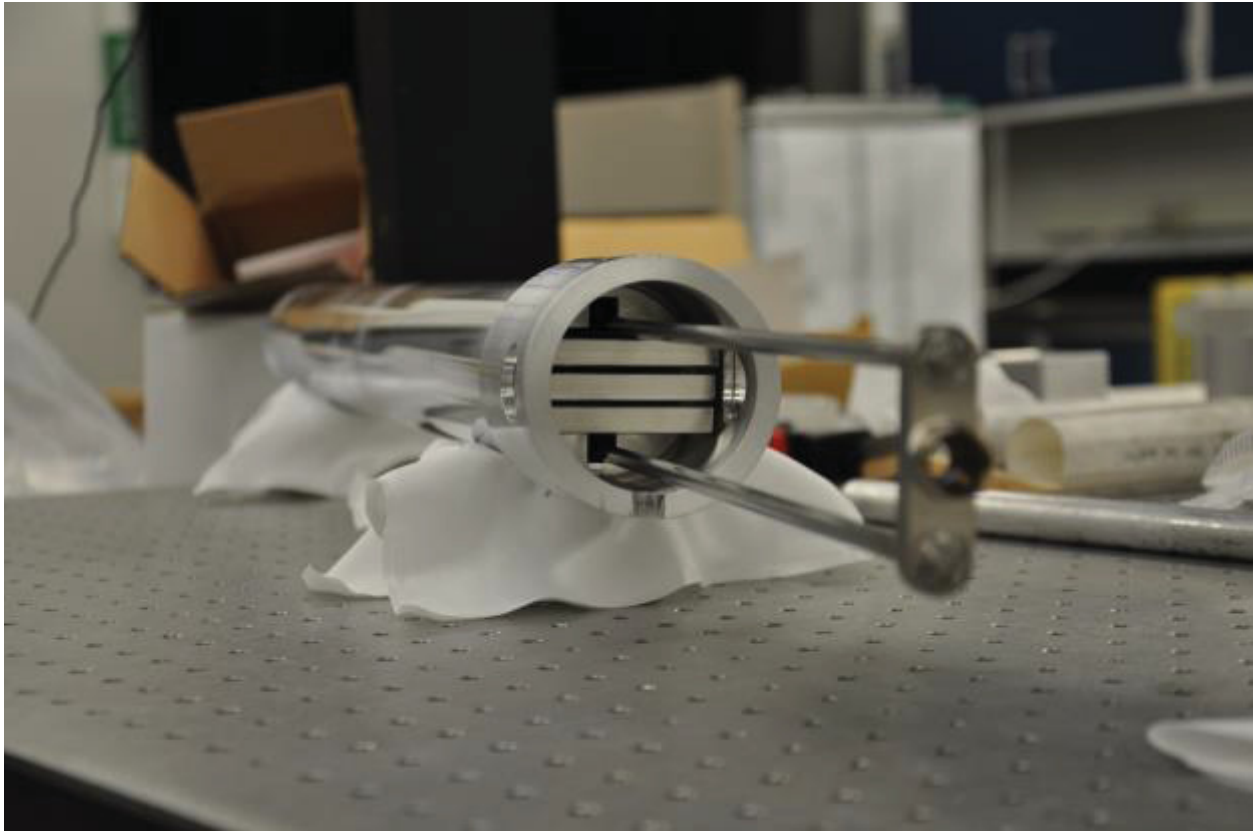


Figure 5. Loaded sample holder with pull rod mechanism extended

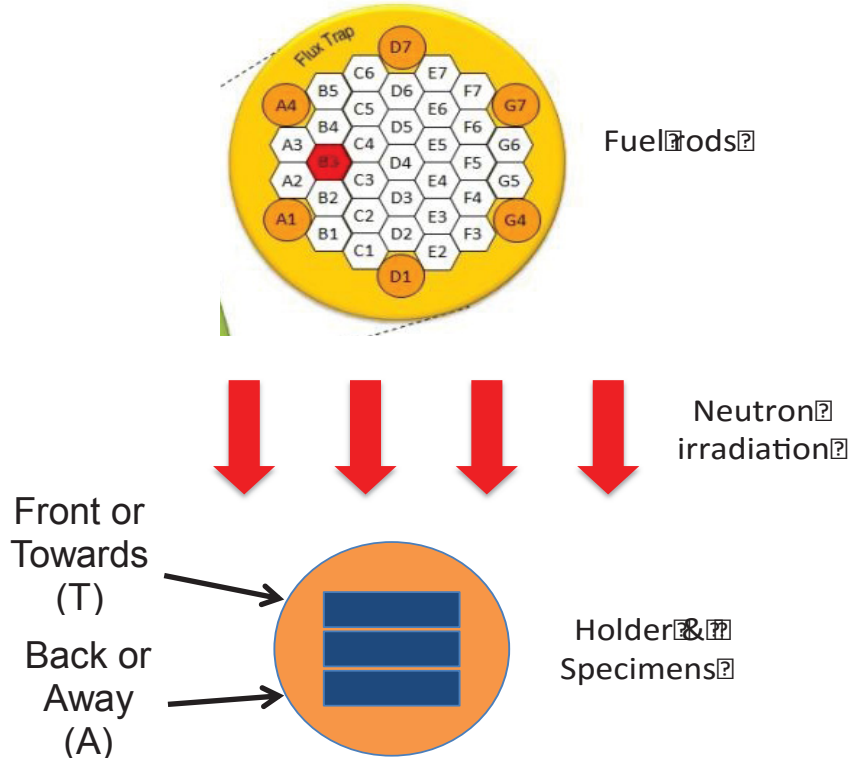


Figure 6. Orientation of the specimens relative to the fuel rod and neutron irradiation

VFP-34			VFP-37			VFP-38		
Front	Middle	Back	Front	Middle	Back	Front	Middle	Back
1471	1471	1471	1471	1471	1471	1471	1471	1471
ORNL-1222-0	ORNL-1222-0	ORNL-1222-0-4	ORNL-1222-0	ORNL-1222-0	ORNL-1222-0	ORNL-1222-0	ORNL-1222-0-8	ORNL-1222-0-3
1471	1471	1471	1471	1471	1471	1471	1471	1471
ORNL-1222-1	ORNL-1222-1	ORNL-1222-1	ORNL-1222-1	ORNL-1222-1	ORNL-1222-1	ORNL-1222-1	ORNL-1222-1	ORNL-1222-1
1471	1471	1471	1471	1471	1471	1471	1471	1471
ORNL-1222-2	ORNL-1222-2	ORNL-1222-2	ORNL-1222-2	ORNL-1222-2	ORNL-1222-2	ORNL-1222-2	ORNL-1222-2	ORNL-1222-2
1471	1471	1471	1471	1471	1471	1471	1471	1471
ORNL-1222-3	ORNL-1222-3	ORNL-1222-3	ORNL-1222-3	ORNL-1222-3	ORNL-1222-3	ORNL-1222-3	ORNL-1222-3	ORNL-1222-3
1471	1471	1471	1471	1471	1471	1471	1471	1471
ORNL-1222-4	ORNL-1222-4	ORNL-1222-4	ORNL-1222-4	ORNL-1222-4	ORNL-1222-4	ORNL-1222-4	ORNL-1222-4	ORNL-1222-4
	EPRI-04			EPRI-05			EPRI-06	

All loaded as shown.
 Jh. Pily 12.6.2014

Figure 7. Loading Diagram for the second irradiation campaign

Helium Level Determination in Neutron Irradiated Stainless Steel

Thermal Desorption Spectrometry (TDS) is a powerful tool to investigate gas behavior in nuclear materials research. A detailed description of the technique was included in Milestone M3LW-17OR0406012 report in June 2017.

Thermal desorption spectrometry (TDS) technique was used to obtain the total amount of helium in the unirradiated 304 stainless steel sample, which requires melting the sample of interest to release all the contained helium. This sample was supplied by EPRI and was produced by powder metallurgy and contained an unknown amount of helium. A new customized resistivity heater with a maximum temperature of 1650°C has been installed to the TDS system located in the LAMDA facility at ORNL. A sample with a weight of 0.12067g was placed in the specially-designed tungsten crucible and then heated to a maximum temperature of 1525°C. The desorbed helium during the temperature ramping process was captured by using a quadrupole mass spectrometer. Figure 8 shows the helium desorption flux as a function of time as well as the temperature profile used in the experiment. The helium desorption is a collective effect of complicated helium-defect interactions within the sample during the thermal annealing process [1]. It is apparent that significant helium desorption occurred starting from 600°C and the major helium release area ranges from 600°C to 1450°C, consisting of three major helium release peaks. The first peak, 600°C to ~1000°C, was attributed to the helium dissociation from weak trapping sites in the sample, like dislocation lines and over-pressurized helium bubbles with high He/V ratio. The most significant helium desorption peak was observed from 1000°C to 1350°C, resulting from the dissociation of a large number of He-V clusters or helium bubbles within the sample due to the high thermal drive force. The sharp helium release peak around 1435°C refer to the melting of the studied materials, enabling the complete release of the contained helium from the sample.

It is noted that the output of the mass spectrometer is in the form of electrical current with a unit of ampere (A) by the mass spectrometer. A calibration process is required to convert the electrical current to the atomic number of helium. A standard helium leak apparatus with known constant gas leakage rate (3.80×10^{-13} mol/s), fabricated by VTI Vacuum Technology, Inc., was used to calibrate the mass spectrometer signals. The conversion coefficient obtained from the calibration process is 0.0998 mol/C. Therefore, the integral of the total desorbed helium is 2.45×10^{-7} mol. Given the mass of the sample (0.12067 g) and other basic parameters (density: 8 g/cm³, 7 cm³/mol), the helium concentration in this sample is determined to be 111.25 appm.

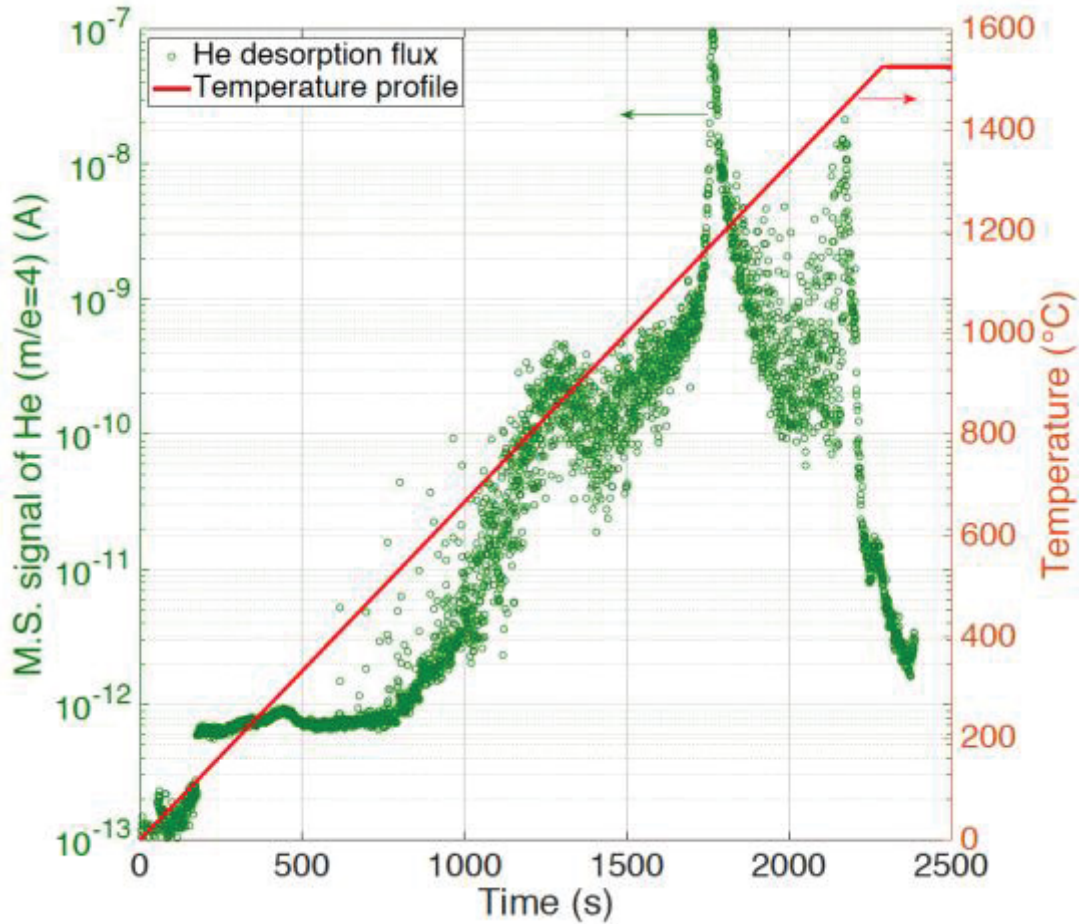


Figure 8. Helium desorption flux as a function of time during the thermal annealing process of unirradiated He-containing 304SS sample. The temperature profile is shown as a red line

Helium Distribution in Neutron Irradiated Stainless Steel

Four irradiated stainless steel specimens were sectioned and prepared for atomic scale chemistry analysis via atom probe tomography (APT). The specimens were taken from the materials inventory that was generated during the first HFIR irradiation campaign of the irradiated materials welding test program. Types 304L and 316L stainless steel with nominal target helium contents of 10 appm and 30 appm were selected from the inventory. Electron backscatter diffraction was used in tandem with focused ion beam (FIB) milling at ORNL's LAMDA facility to selectively remove high angle grain boundaries from each specimen for APT analysis. One FIB lift-out was removed from a high angle grain boundary from each specimen and transferred to the University of Michigan, where APT analysis is currently underway. Identifying ^{10}B , ^{11}B , and ^7Li distributions is of particular interest in the samples as the HFIR irradiation conditions were selected to fully transmute all ^{10}B in the specimens via a (n,a) reaction which produces ^7Li . The presence or lack of ^7Li along microstructural features can be used as an indication of the He distribution within the materials. A representative APT mass spectrum from 304L showing natural and observed isotopic distribution of ^{10}B , ^{11}B , and ^7Li is presented in Figure 9. An example APT grain boundary reconstruction from 304L and resulting grain boundary solute profiles are presented in Figures 10 and 11, respectively.

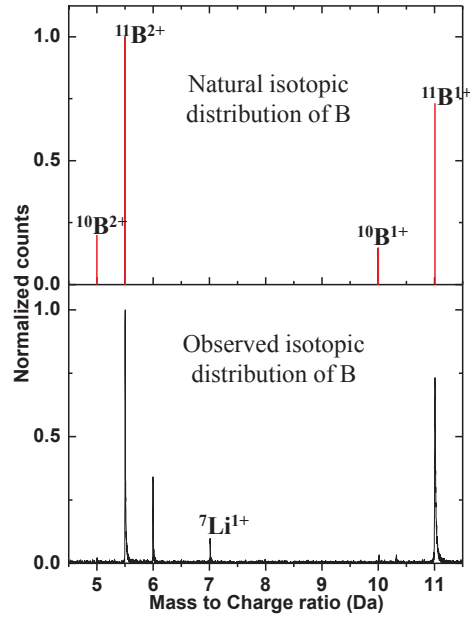


Figure 9. Representative mass spectrum from 304 SS showing natural and observed isotopic distribution of peaks for ^{10}B and ^{11}B

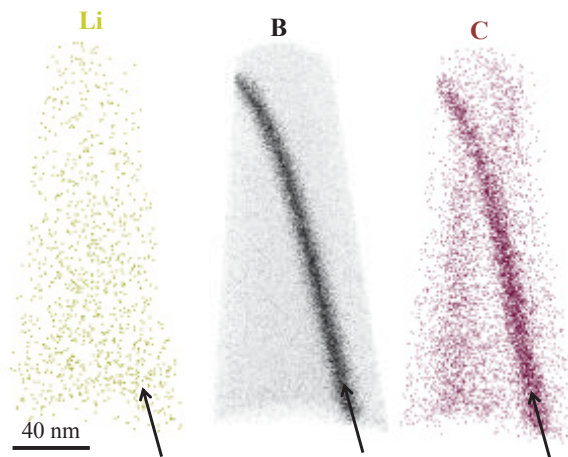


Figure 10. Representative reconstructed datasets from the neutron irradiated 304C sample showing distribution of Li, B and C along high angle grain boundary. Arrow indicates location of grain boundary in the 3-D reconstructed volume

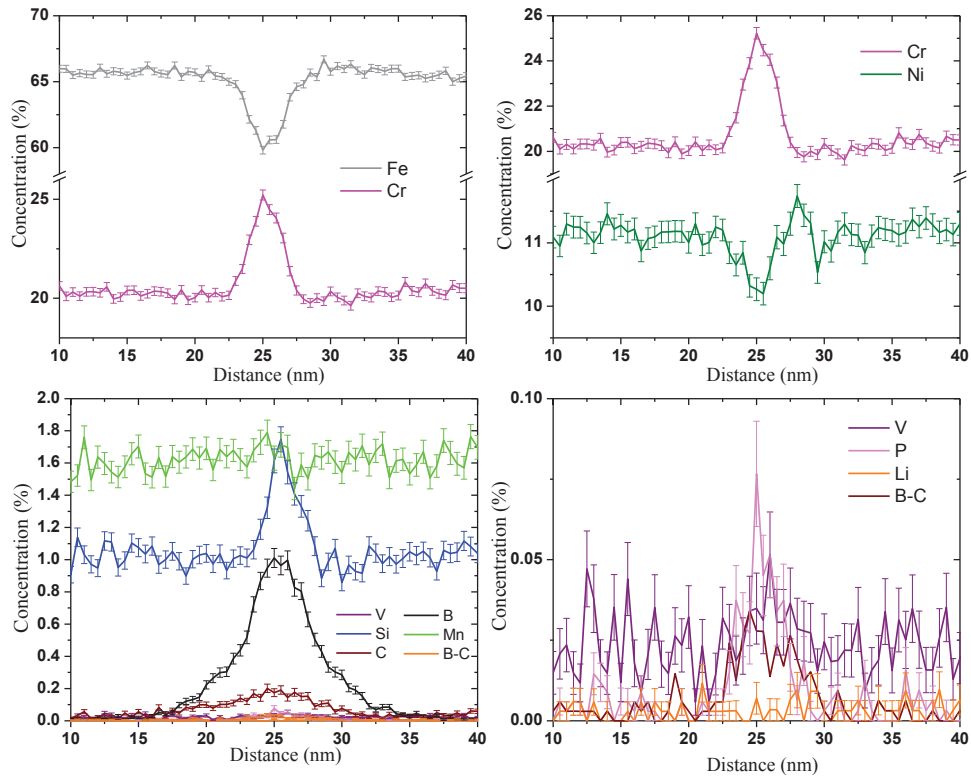


Figure 11. Representative 1-D profile across the high angle grain boundary from the neutron irradiated 304C sample showing distribution of all elements

Planning for Additional Irradiations

Table 3 summarizes the number of specimens available for testing and/or welding with respect to the alloy identification, the end date of the irradiation campaign material, and material condition (wrought or weld microstructure). Analysis of the first irradiation campaign indicated that it can be assumed that the helium concentration is essentially the same as the starting boron level indicating complete transmutation of the boron to helium.

The assessment of the total number of coupons available for welding and an evaluation by EPRI on potential helium levels in existing reactor materials and radiation history indicated that production of additional coupons is needed for critical helium levels and that it was advisable to produce coupons with even higher potential helium levels than produced in the past. A campaign was started to produce four additional material heats that that will provide additional coupons comparable to previously made material (304C, 304E, 316C, 316E) plus two heats of material (304L and 316L) with higher helium generation potential that will irradiated at a later date in the HFIR facility. The two higher helium generation potential heats are targeted to contain 50 ppm by weight natural boron. EPRI located a source and supplied low cobalt 304L stainless rod material to produce the planned six heats. This rod stock was of a smaller diameter (~ 22 mm) than previously used and required a new electrode design for VAR processing. Figure 12 is the electrode design to produce a heat 316L stainless steel with controlled boron. To produce the controlled boron level in 316L from the 304L starting material, three pieces of the 304L barstock (item 2) are assembled by welding with Nickel 270 rods (item 4), pure Molybdenum rods (item

5) and 304L master heat containing 1.82% natural boron (item 3) to produce an electrode assembly. The amount of boron containing master alloy is adjusted to produce targeted boron levels for each heat. The electrodes for borated 304L are very similar but with the omission of the Nickel and Molybdenum rods. Figure 13 is a photograph of the six electrodes assemblies prepared for VAR processing. Figure 14 shows the as produced 89 mm diameter casting from VAR processing. After removal of the hot top section and base to solid material, the castings were extruded through a 19 by 51 mm rectangular die opening after heating to 1100 °C. The extrusions were cut into sections to enable cross rolling, forged flat and machined on the faces and are shown in Figure 15.

Five of the six new heats have completed electrode fabrication, VAR processing, flattening and rough machining and are ready for homogenizing and hot rolling. A gas evolution problem occurred in the new heat equivalent to 316C during VAR processing that caused a loss of vacuum, VAR shutdown and loss of the electrode. The resulting casting was considered too small to produce adequate finished rolled bar. A new electrode to replace this heat was prepared. This electrode also failed due to melting in the center of the stub end of the electrode and caused it to fall into in the partially completed casting. Further work on a replacement electrode as well as final processing of the extrusion sections shown in Figure 15 has been placed on hold due to funding limitations.

Table 3. Available irradiation specimens for welding or helium analysis

Alloy and Boron Level	Microstructure Wrought/Weld	Irradiation Campaign 1 Completed June 2014 Number of Specimens	Irradiation Campaign 2 Completed May 2017 Number of Specimens
304A	Wrought	4	1
304B	Wrought	4	1
304C	Wrought	5	1
304D	Wrought	5	1
304E	Wrought	5	1
316A	Wrought	3	1
316B	Wrought	4	2
316C	Wrought	5	2
316D	Wrought	5	1
316E	Wrought	5	
182A	Wrought		4
182B	Wrought		4
182C	Wrought		4
182D	Wrought		4
182E	Wrought		4
182D	Weld		7
182E	Weld		7

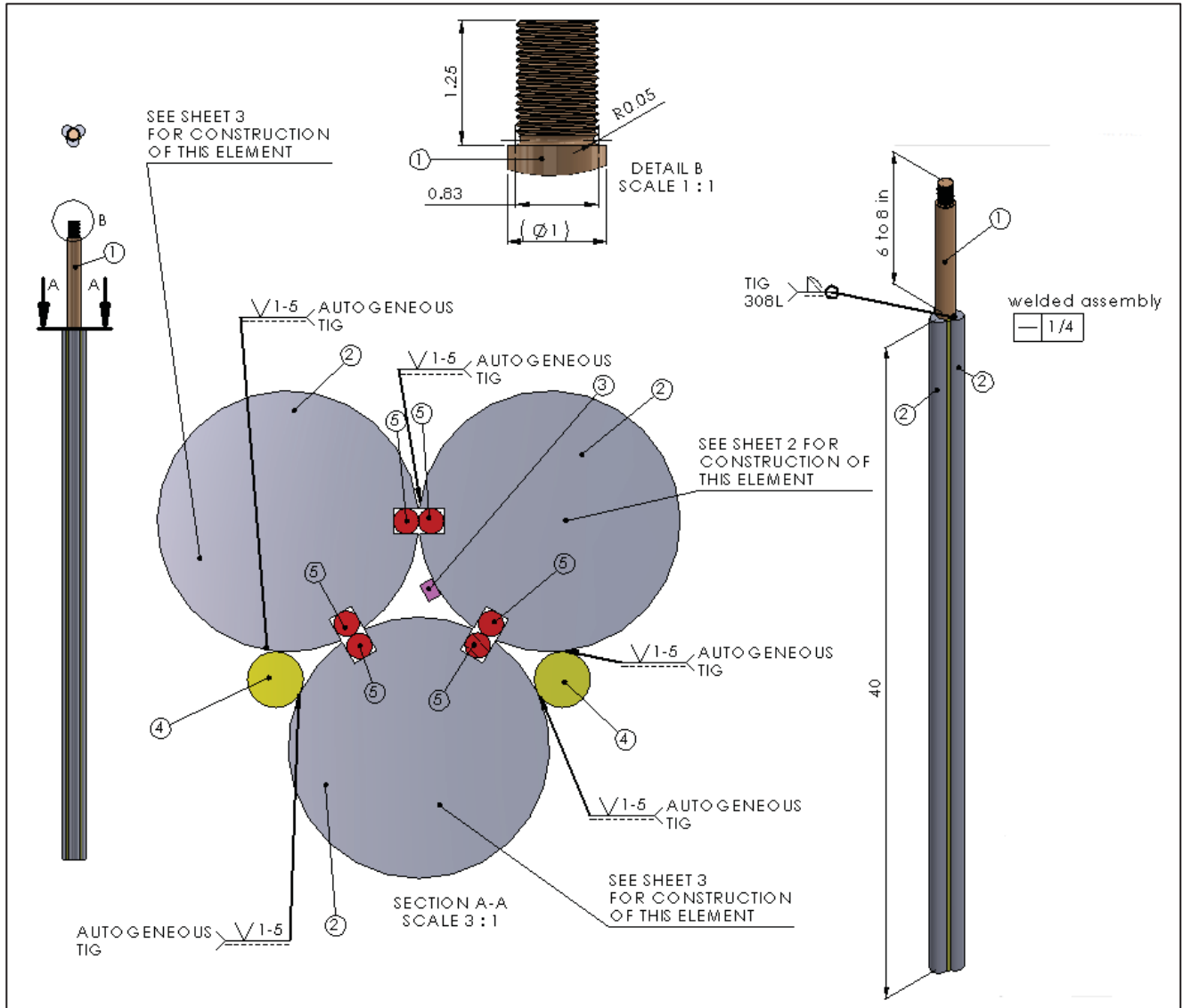


Figure 12. Electrode design for producing 316L with controlled boron levels



Figure 13. Electrode Assemblies of 304L and 316L with controlled boron additions prior to VAR processing



Figure 14. Completed VAR casting and remaining electrode stub



Figure 15. Extruded and cut billets ready for hot rolling

References

- [1] X. Hu, D. Xu, and B. D. Wirth, *Journal of Nuclear Materials* **442**, S649 (2013).